ChemComm

COMMUNICATION

View Article Online
View Journal | View Issue

Cite this: *Chem. Commun.*, 2022, **58**, 8282

Received 24th May 2022,
Accepted 28th June 2022

DOI: 10.1039/d2cc02931f

rsc.li/chemcomm

Stereoselective insertion of cyclopropenes into Mg–Mg bonds†

Feriel Rekhroukh,‡[a] Linxing Zhang, ‡[ab] Richard Y. Kong, [a] Andrew J. P. White[a] and Mark R. Crimmin *[a]

The reaction of cyclopropenes with compounds containing Mg–Mg bonds is reported. 1,2-Dimagnesiation occurs exclusively by *syn*-addition to the least hindered face of the alkene forming a single diastereomeric product. DFT calculations support a concerted and stereoselective mechanism. These findings shed new light on the stereochemistry of reactions involving magnesium reagents.

The direct functionalisation of alkenes is an essential component of modern organic chemistry. Since the pioneering contribution of Markovnikov,[1] it has been clear that controlling the selectivity of this reaction is of vital importance. While the regioselectivity of alkene functionalisation can be determined by assignment of the reaction products, for simple linear alkenes the stereoselectivity (*syn- vs. anti*-addition) is often a hidden consideration. In this regard, cyclic alkenes – specifically cyclopropenes – offer an opportunity to study the stereochemistry of alkene functionalisation.

Protocols for the hydroelementation and carboelementation of cyclopropenes have been reported. For example, a number of selective catalytic methods for the hydroboration,[2,3] hydrostannation,[4] and hydrosilylation[5] of cyclopropenes have emerged in the recent years. Similarly, selective catalytic carbozincation[6,7] and carbomagnesiation[8] reactions of cyclopropenes have been achieved. These reactions typically employ organozinc or organomagnesium compounds in combination with a transition metal catalyst. In almost all cases, exclusive *syn*-addition to the cyclopropene occurs to give a single diastereomer, suggestive of a concerted and stereospecific transition state for carbometallation. Direct isolation and structural characterisation of the organometallic intermediates in these reactions is, however, uncommon; they are usually subjected to subsequent synthetic transformations without isolation.

Very recently the scope of main group reagents that can be used to functionalise alkenes has been expanded to compounds that contain reactive Mg–Mg bonds.[9–11] Both Jones and coworkers,[12–14] and our group,[15] have demonstrated the 1,2-dimagnesiation of alkenes. In specific cases the reaction has been shown to be reversible. Despite the importance of these findings, the stereochemistry of addition remains unknown. In this paper, we report the 1,2-dimagnesiation of cyclopropenes. For the cases investigated, the reaction is stereoselective and occurs by *syn*-addition to the least hindered face of the cyclopropene. DFT calculations support a concerted reaction mechanism. We also investigate the stereointegrity of the resulting organomagnesium compounds. Despite the known propensity of stereocentres adjacent to Mg to undergo epimerisation,[16–26] the *syn*-addition products are stable up to 60 °C.

Reaction of **1a** with cyclopropene **2a**, at 25 °C in C_6D_6 led to the rapid formation of the 1,2-dimagnesiocyclopropyl complex **3a**. Similar reactivity was observed between **1a** and **2b** (15 min at 25 °C) or **2c** (4 h at 60 °C), leading to the corresponding species **3b** and **3c**. The slowest reaction occurs with the most sterically hindered substrate. In all cases, the selective *syn*-insertion of the alkene into the Mg–Mg bond was observed. For **2a** and **2b**, attack of **1a** occurs on the least hindered face of the ring system leading to the formation of a single diastereomer of the product (Scheme 1).

Isolation and characterisation of **3a-c** was possible by further reaction with either DMAP or THF to form **3a**·**(DMAP)$_2$**, **3b**·**(THF)$_2$**, and **3c**·**(THF)$_2$**. NMR spectroscopic data are consistent with symmetric structures. The most salient NMR data are the ^{1}H and ^{13}C signals observed for methine position directly linked to the Mg centre, which are observed in the following ranges: δ_H = −0.19 to −0.70 ppm and δ_C = 33.1 to 35.1 ppm. The structure of **3a**·**(DMAP)$_2$** was confirmed by X-ray diffraction analysis (Fig. 1a). The extremely long Mg–Mg separation

[a] *Department of Chemistry, Molecular Sciences Research Hub, Imperial College London, 82 Wood Lane, Shepherds Bush, London, W12 0BZ, UK. E-mail: m.crimmin@imperial.ac.uk*
[b] *Shenzhen Bay Laboratory, Shenzhen, 518132, P. R. China*

† Electronic supplementary information (ESI) available: Experimental procedures, details of calculations and characterization data (PDF). Coordinates for DFT calculations (*xyz*). Crystallographic data for **3a**·**(DMAP)$_2$** and **4c**·**(DMAP)$_2$** (cif). CCDC 2173920 and 2173921. For ESI and crystallographic data in CIF or other electronic format see DOI: https://doi.org/10.1039/d2cc02931f

‡ Joint 1st authors.

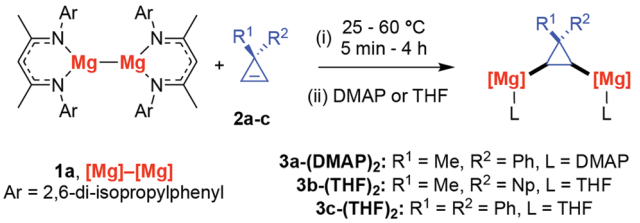

Scheme 1 Stereoselecive 1,2-dimagnesiation of cyclopropenes.

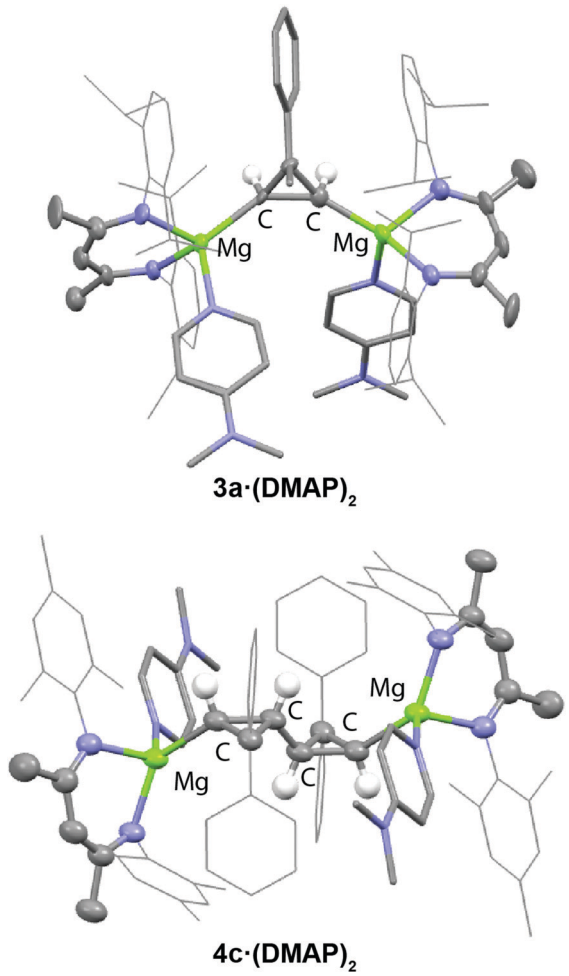

Fig. 1 Structures of **3a**·**(DMAP)$_2$** and **4c**·**(DMAP)$_2$** from single crystal X-ray diffraction experiments.

(>5.0 Å) along with the single bond C(1)–C(2) distance of 1.57(1) Å are consistent with the proposed insertion reaction. The Mg–C bonds of 2.02(1) and 2.20(1) Å are in the normal range for magnesium alkyls.[12] Additional support for the proposed structure being retained in solution was obtained through *in situ* generation of an asymmetric analogue of **3a** (with different ligands on each Mg centre). In this case, the two protons of the cyclopropane moiety become inequivalent. Analysis of the ^{1}H NMR spectrum of the crude reaction mixture indicates a mutual $^3J_{HH}$ = 13.6 Hz coupling for the cyclopropane protons which is consistent with known literature values for *syn*-stereochemistry.[27]

Addition of **2a-c** (2 equiv.) to **1b**, a less sterically hindered analogue of **1a**, also proceeded extremely rapidly at 25 °C in C_6D_6 solution to form a single diastereomeric product. In these cases, however, a double insertion reaction occurred, forming **4a-c** (Scheme 2). This reaction likely proceeds by two sequential steps: (i) a *syn*-selective insertion of the cyclopropene into the Mg–Mg bond of **1b** and (ii) a *syn*-selective carbomagnesiation of a second equivalent of cyclopropene from the intermediate 1,2-dimagnesiocyclopropyl complex. This type of reactivity has already been reported by Jones and co-workers for reaction of **1b** with ethylene in the presence of an N-heterocyclic carbene ligand.[14] In the case of **2c**, an intermediate **3d** could be spectroscopically observed. Addition of a further equiv. of cyclopropane to this intermediate led to **4c**.

The isolation of **4a-c** was again achieved by reaction with DMAP. **4a-c**·**(DMAP)$_2$** were isolated as yellow powders by precipitation in *n*-hexane in 50–75% yield. Spectroscopic data are consistent with their formulation. For example, for **4c**·**(DMAP)$_2$**, is characterised by two sets of doublets in the high field region of the ^{1}H NMR spectrum at δ = 0.22 (2H, $^3J_{HH}$ = 10.5 Hz) and δ = 1.30 (2H, $^3J_{HH}$ = 10.5 Hz) ppm. The mutual coupling between these resonances was confirmed by a COSY NMR experiment. Clear evidence for the *syn*-selective double insertion is also evident from single-crystal X-ray diffraction of **4c**·**(DMAP)$_2$** (Fig. 1b).

To gain a deeper understanding of the stereochemistry a series of plausible mechanisms were investigated by DFT calculations using the B3PW91 functional.[28] Prior DFT studies have modelled the addition of ethylene to a derivative of **1b**, but stereochemistry was not a consideration in this case.[14] The reaction of **1b** with cyclopropene **2a** is calculated to proceed by an initial formation of a weak van der Waals complex **Int-1** followed by a stereoselective *syn*-addition transition state **TS-1** that connects directly to the product **Int-2** (Fig. 2). **Int-2** (R^1 = Me, R^2 = Ph) is a direct analogue of the spectroscopically observed intermediate **3d** (R^1 = R^2 = Ph). This reaction is predicted to be exergonic by ΔG° (298 K) = –29.0 kcal mol^{-1} with a readily accessible activation barrier of $\Delta G^\ddagger$ (298 K) = 5.7 kcal mol^{-1}. An alternative *syn*-addition pathway in which **1b** approaches the more hindered face of **2a** was calculated to proceed by a slightly higher energy transition state **TS-2** ($\Delta G^\ddagger$ (298 K) = 9.3 kcal mol^{-1}). The concerted *anti*-addition pathway, while leading to the most thermodynamically stable product, ΔG° (298 K) = –34.2 kcal mol^{-1}, is prohibitively high in energy requiring distortion of the reactants into a twisted geometry in **TS-3** ($\Delta G^\ddagger$ (298 K) = 30.7 kcal mol^{-1}). Hence, the calculations are consistent with the experiments and predict that the reaction of **1b** with **2a** should be under kinetic control and highly stereoselective at room temperature ($\Delta\Delta G^\ddagger$ (298 K) = 3.6 kcal mol^{-1}).

Comparison of **TS-1**, **TS-2**, and **TS-3** explains the origin of *syn*-selectivity. **TS-1** is a four-membered transition state, and its structure determines the *syn*-addition to the least hindered face of the alkene. The geometry of **TS-1** is asymmetric with one short Mg^1–C^1 (2.48 Å) and one long Mg^2–C^2 (3.08 Å) bond. **TS-2**

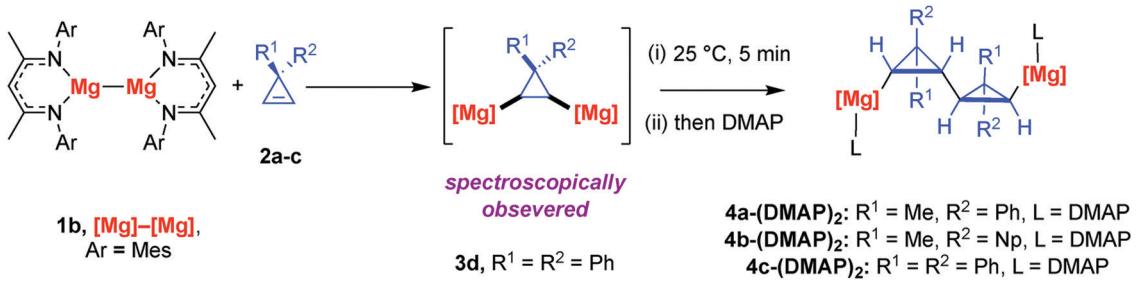

Scheme 2 Sequential 1,2-dimagnesiation and carbometallation of cyclopropenes.

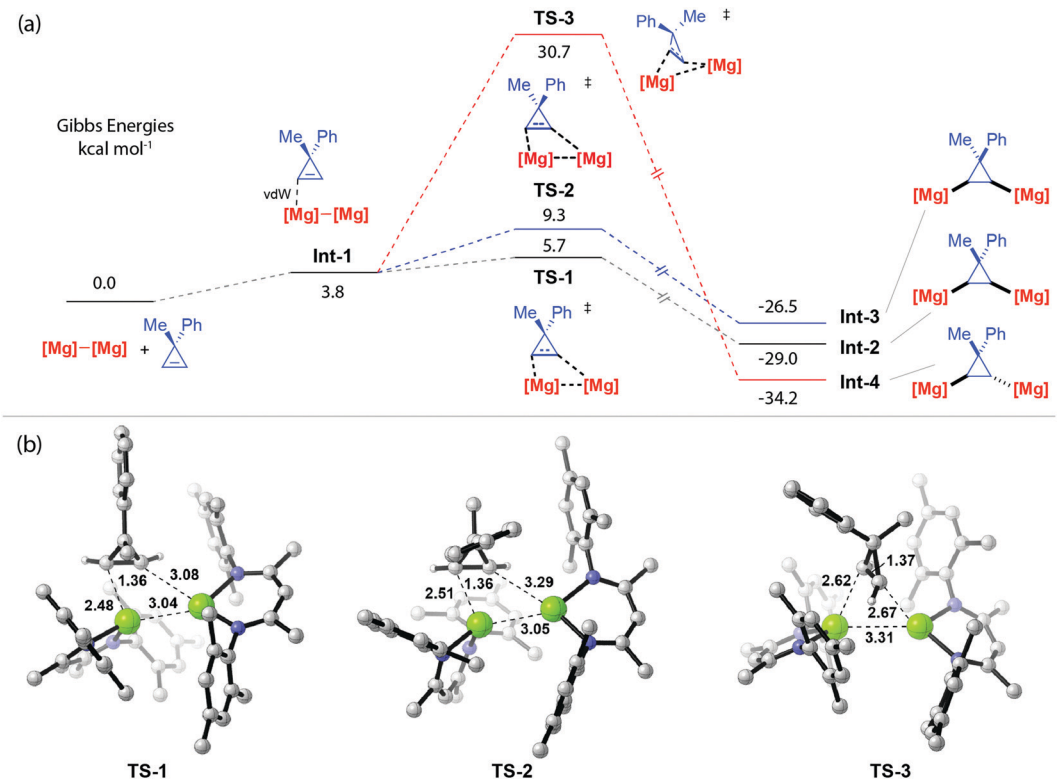

Fig. 2 (a) Free energy profile for mechanism of the first insertion. (b) Geometries of first insertion trasition states **TS1-Me**, **TS1-Ph** and **TS1-anti**. Computed at the PCM (benzene)/B3PW91-D3(BJ)/def2-TZVP//B3PW91/SDDAll-6-31G(d,p) level.

is similar. NBO calculations are also consistent with asynchronous bond formation occurring in **TS-1**, as evidenced by analysis of the NPA charges, which develop asymmetrically for both pairs of magnesium and carbon atoms (Fig. 3). The data indicate that the Mg^1–C^1 bond is formed earlier than the Mg^2–C^2 bond. In contrast, **TS-3** is more symmetric, with almost no difference in two Mg–C bond distances (2.62 Å and 2.67 Å). This closer approach of the Mg–Mg reagent, combined with the required antarafacial bond formation to the π-system strongly disfavour the *anti*-addition by **TS-3**.

Further comparison of **TS-1** and **TS-2** can be used to rationalise the facial selectivity. QTAIM calculations combined with non-covalent interaction (NCI) analysis for reveals that **TS-1** is stabilised by a greater number of (π-H–C) non-covalent interactions than **TS-2** (Fig. 4). While we have not quantified these, it is likely a balance between these attractive dispersion interactions,[29] and steric repulsion that favours addition to the face with the methyl substituent. The DFT model was expanded to consider chemoselectivity (see Fig. S30, ESI†). To simplify the possible reaction outcomes the substrate was modified to avoid the complication of facial selectivity. Calculations suggest that the *syn*-addition of two equiv. of the diphenyl substituted cyclopropene **2c** to **1b** to form the double insertion product **4c** is energetically feasible. The first insertion occurs with a barrier of $\Delta G^{\ddagger}$ (298 K) = 6.6 kcal mol^{-1}, the second with a barrier of $\Delta G^{\ddagger}$ (298 K) = 15.8 kcal mol^{-1}, the overall reaction is exergonic by ΔG° (298 K) = −80.5 kcal mol^{-1}. Hence, while the barrier to the second *syn*-insertion is higher than the first, both

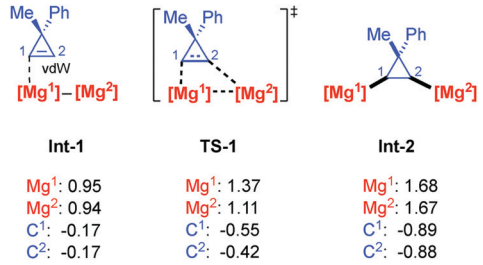

Fig. 3 NPA charges of the Me-facial *syn*-selective insertion **Int-1**, **TS-1** and **Int-2**. Computed at the PCM (benzene)/B3PW91-D3(BJ)/def2-TZVP//B3PW91/SDDAll-6-31G(d,p) level.

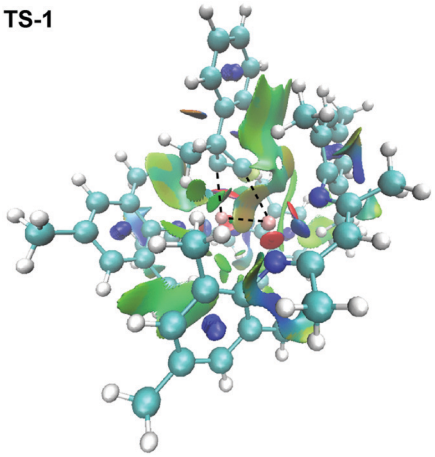

Fig. 4 NCI plot of transition state **TS-1**.

are expected to be accessible under the experimental conditions.

Isolation of **3b**·$(THF)_2$ - an organomagnesium compound with a defined stereochemistry – provides an opportunity to investigate the stereointegrity of centres adjacent to the magnesium site. Prior solution studies suggest that 2° alkyl magnesium reagents show increased configuration stability over 1° analogues.[16–18,21,23,26] 2° Alkyl magnesium reagents bearing cyclopropyl groups are expected to be the most stable derivatives, due to the low p-character of the α-carbon.[19,20] For example, the half-life of racemisation of an enantiopure nitrile-substituted cyclopropyl magnesium reagent has been measured as 11 h at –100 °C[22,24,25] in Et_2O. **3b** is formed under kinetic control due to the *syn*-addition pathway described above. The *anti*-isomer is expected to be thermodynamically more stable based on steric grounds. Monitoring 13.8 mM concentration solutions of **3b**·$(THF)_2$ in C_6D_6 solution over 120 h at 25 °C and then 120 h at 60 °C provided no evidence for epimerisation. The data suggest that **3b** retains a *syn*-stereochemistry up to modest temperatures and that epimerisation in this system is not facile.

In summary, we have developed an experimental and computational understanding of the stereochemistry of 1,2-dimagnesiation of cyclopropenes. Key to this understanding is the realisation that the reaction occurs by a concerted *syn*-addition transition state in which the Mg–Mg bond adds across the most sterically accessible face of the alkene. These findings may have broad implications for the design of stereoselectivity reactions involving the addition of magnesium reagents to unsaturated carbon–carbon and carbon–heteroatom bonds.

We are grateful to the Leverhulme Trust for Funding (RPG 2020-006) and China Scholarship Council (CSC) for support.

Conflicts of interest

There are no conflicts to declare.

Notes and references

1 W. Markownikoff, *Justus Liebigs Ann. Chem.*, 1870, **153**, 228–259.
2 M. Rubina, M. Rubin and V. Gevorgyan, *J. Am. Chem. Soc.*, 2003, **125**, 7198–7199.
3 A. F. Littke, C. Dai and G. C. Fu, *J. Am. Chem. Soc.*, 2000, **122**, 4020–4028.
4 M. Rubina, M. Rubin and V. Gevorgyan, *J. Am. Chem. Soc.*, 2004, **126**, 3688–3689.
5 L. Dian and I. Marek, *Org. Lett.*, 2020, **22**, 4914–4918.
6 M. Nakamura, A. Hirai and E. Nakamura, *J. Am. Chem. Soc.*, 2000, **122**, 978–979.
7 D. S. Müller and I. Marek, *J. Am. Chem. Soc.*, 2015, **137**, 15414–15417.
8 Y. Cohen and I. Marek, *Angew. Chem., Int. Ed.*, 2021, **60**, 26368–26372.
9 S. P. Green, C. Jones and A. Stasch, *Science*, 2007, **318**, 1754–1757.
10 S. J. Bonyhady, C. Jones, S. Nembenna, A. Stasch, A. J. Edwards and G. J. McIntyre, *Chem. – Eur. J.*, 2010, **16**, 938–955.
11 C. Jones, *Nat. Rev. Chem.*, 2017, **1**, 0059.
12 A. J. Boutland, A. Carroll, C. Alvarez Lamsfus, A. Stasch, L. Maron and C. Jones, *J. Am. Chem. Soc.*, 2017, **139**, 18190–18193.
13 D. Dange, A. R. Gair, D. D. L. Jones, M. Juckel, S. Aldridge and C. Jones, *Chem. Sci.*, 2019, **10**, 3208–3216.
14 K. Yuvaraj, I. Douair, L. Maron and C. Jones, *Chem. – Eur. J.*, 2020, **26**, 14665–14670.
15 R. Y. Kong and M. R. Crimmin, *J. Am. Chem. Soc.*, 2020, **142**, 11967–11971.
16 G. M. Whitesides and J. D. Roberts, *J. Am. Chem. Soc.*, 1965, **87**, 4878–4888.
17 G. M. Whitesides, M. Witanowski and J. D. Roberts, *J. Am. Chem. Soc.*, 1965, **87**, 2854–2862.
18 M. Witanowski and J. D. Roberts, *J. Am. Chem. Soc.*, 1966, **88**, 737–741.
19 H. M. Walborsky, F. J. Impastato and A. E. Young, *J. Am. Chem. Soc.*, 1964, **86**, 3283–3288.
20 H. M. Walborsky and A. E. Young, *J. Am. Chem. Soc.*, 1964, **86**, 3288–3296.
21 R. W. Hoffmann, *Chem. Soc. Rev.*, 2003, **32**, 225.
22 P. R. Carlier and Y. Zhang, *Org. Lett.*, 2007, **9**, 1319–1322.
23 J. Beckmann and A. Schütrumpf, *Org. Biomol. Chem.*, 2009, **7**, 41–42.
24 N. N. Patwardhan, M. Gao and P. R. Carlier, *Chem. – Eur. J.*, 2011, **17**, 12250–12253.
25 P. J. Rayner, P. O'Brien and R. A. J. Horan, *J. Am. Chem. Soc.*, 2013, **135**, 8071–8077.
26 S. Koller, J. Gatzka, K. M. Wong, P. J. Altmann, A. Pöthig and L. Hintermann, *J. Org. Chem.*, 2018, **83**, 15009–15028.
27 H. M. Hutton and T. Schaefer, *Can. J. Chem.*, 1963, **41**, 684–689.
28 M. J. Frisch, *et al.*, Geometry optimizations were carried out using the B3PW91/SDDAll-6-31G(d,p). Single-point calculations were performed at SMD (benzene)/B3PW91-D3(BJ)/def2-TZVP-6-311+G(d,p) level. All calculations were conducted with Gaussian09, Gaussian, Inc., Wallingford CT, 2009. More details are included in the ESI.
29 D. J. Liptrot, J. Guo, S. Nagase and P. P. Power, *Angew. Chem., Int. Ed.*, 2016, **55**, 14766–14769.